scientific reports

Check for updates

OPEN

Entropy generation analysis for MHD flow of water past an accelerated plate

Tarek N. Abdelhameed

This article examines the entropy generation in the magnetohydrodynamics (MHD) flow of Newtonian fluid (water) under the effect of applied magnetic in the absence of an induced magnetic field. More precisely, the flow of water is considered past an accelerated plate such that the fluid is receiving constant heating from the initial plate. The fluid disturbance away from the plate is negligible, therefore, the domain of flow is considered as semi-infinite. The flow and heat transfer problem is considered in terms of differential equations with physical conditions and then the corresponding equations for entropy generation and Bejan number are developed. The problem is solved for exact solutions using the Laplace transform and finite difference methods. Results are displayed in graphs and tables and discussed for embedded flow parameters. Results showed that the magnetic field has a strong influence on water flow, entropy generation, and Bejan number.

List of symbols

A	Acceleration of the plate, (ms^{-2})
v	Velocity of the fluid, (ms^{-1})
ϑ	Temperature of the fluid, (K)
g	Acceleration due to gravity, (ms^{-2})
B_0	Applied magnetic field
c_p	Specific heat at a constant pressure, (J kg^{-1} K^{-1})
Gr	Thermal Grasshof number, (–)
k	Thermal conductivity of the fluid, (W m^{-2} K^{-1})
Nu	Nusselt number, (–)
Pr	Prandtle number, ($= \mu c_p/k$)
q	Laplace transforms parameter

Greek symbols

μ	Dynamic viscosity, (kg m^{-1}-s^{-1})
ρ	Fluid density, (kg ms^{-3})
β_0	The volumetric coefficient of thermal expansion, (K^{-1})
τ	Time, (s)
θ	Fluid temperature far away from the plate, (K)
σ	Stephen-Boltzmann constant

Entropy plays a very important role in fluid dynamics. The second law of thermodynamics totally revolves around the entropy concepts and entropy generation. The feasibility of a process and its efficiency are directly related to entropy generation in the process. Since entropy generation is much important and happens in all flow processes because of friction in fluids, therefore, in this paper, we study entropy generation in (MHD) the flow of water which is taken as a counter-example of a Newtonian fluid, flows over a second-order accelerated plate taken in the vertical direction. One of the useful applications of entropy generation in real life/world is in the design of systems that rely on heat transfer. Entropy tells us in a way, the best we can do to avoid thermal energy losses.

[1]Basic Engineering Sciences Department, College of Engineering, Majmaah University, Majmaah 11952, Saudi Arabia. [2]Mathematics Department, Faculty of Science, Beni-Suef University, Beni-Suef 62514, Egypt. email: t.ahmed@mu.edu.sa

Amongst the various researchers working on entropy generation, the most famous is true, Adrian Bejan, who has published many kinds of research on entropy generation and the second law of thermodynamics with applications in various fields, see for example[1–7].

The importance of entropy generation-EG (second law of thermodynamics-SLTD) in examining heated fluid flows in several engineering devices of practical use and heat related systems has become significant. For example, in thermal analyses, one can see that a worth paying attention part of energy is wasted during the heat transfer and not producing the desired result. Indeed, the scientists were not happy with such a great loss of energy and finally they realized that such energy losses can be removed or minimized by properly designing the heat system. Entropy generation-EG can be produced by several means for instance, heat transfer in thermal systems. Some important key sources amongst the many others, from which Entropy generation-EG in thermal systems include viscous dissipation, chemical reaction, mass transfer, heat transfer, and electrical conduction[8]. In the interesting work of Awed[9], he introduced a new definition of the Bejan number(BN). The BN is indeed, useful in several cases, as it can clearly provide evidence related the dominance of a strong magnetic field and corresponding fluid friction entropy via heat transfer, or vice versa. Saouli and Aïboud-Saouli[10] examined entropy generation-EG in a liquid film such that it is falling along with plate inclided along the plane. A great work for the interesting analysis of entropy generation-EG for the famous Tiwari and Das model was developed by Sheremet et al.[11]. In their study the carefully examined the process and examined some interesting and important computational results for finding the solution to their problem. In their investigation, they examined carefully that addition of nanoparticles in a regular base fluid, the heat transfer rate enormously increased and, then consequently, the cavity of convective flow was found much smaller. For turbulence-forced convection, entropy generation-EG was discussed in details in an excellent and interesting work of Ji et al.[12]. However, recently, Qing et al.[13] examined entropy generation-EG for non-Newtonian fluid of Casson model conating nanoparticles inside a regular base fluid in the presence of a strong magnetic field. The analysis was done over a porous surface with a stretching or shrinking sheet to examine MHD flow. A strong comupational technique known as successive linearization method (SLM) was used for solving a strong system of equations and highlighted the influence of various parameters on velocity and temperature. Sheikholeslami et al.[14], numerically examined the impact of Lorentz forces on Fe_3O_4-water ferrofluid entropy and exergy treatment within a permeable semi annulus by applying a strong numerical scheme.

In all the above problems, entropy generation analysis was done using the numerical treatment. Indeed the entropy generation problem via exact treatment is very rare due to the complex mathematical calculi. However, limited studies are available in this direction, including the work of Saqib et al.[15], in which they investigated entropy generation for generalized nanofluids via exact solution treatment. In this paper, the main objective was to examine entropy for fractional partial differential equations. They first formulated the problem and then solved for exact solutions fluid problem with plots and physical interpretations. They noted that the classical solutions can be obtained in a limiting sense for the unit value of the fractional parameter. Khan et al.[16] applied the classical approach for both the formulation and solution and examined the entropy generation in an unsteady MHD flow with a combined influence of heat and mass transfer through a porous medium where the plate they consider is isothermal and ramped wall temperature.

Numerical methods or see for example Refs.[17–30] and any other was used in many papers[31–43] however, very limited studies are reported in which exact and numerical solutions are simultaneously obtained. Therefore, the main task here is to obtain exact and numerical solutions for the entropy generation problem. More exactly, in this work, the focus is on entropy generation due to highly accelerated plate motion in the vertical direction which is not studied in the literature before this. Water is taken as a counter-example of a Newtonian fluid. The Prandtl number for water is taken as 6.2, however, just for variation purpose, some other values are also taken. The problem is first modeled and then the dimensionless analysis is used to get a transformed system. The results problem is solved for the exact solution using the Laplace transform method whereas for numerical technique, the numerical scheme known as finite difference method has been used. Results are computed and then plotted in various plots and discussed in detail. This paper ends with a conclusion at the end.

Description of the problem. Consider the Casson fluid model for the flow of sodium alginate solution over as accelerated plated. Meanwhile, it is assumed at $\tau \leq 0$, the system was at ambient temperature with zero velocity. However, at $\tau = 0^+$, the fluid starts motion with $v(0,\tau) = A\tau^2$, and temperature variated to $\vartheta(0,\tau) = \theta_w$. Hence, convection is taken place. The governing equation of the flow phenomena are given by

$$\rho \frac{\partial v(\eta,\tau)}{\partial \tau} = \mu \frac{\partial^2 v(\eta,\tau)}{\partial \eta^2} + \rho g \beta_0 (\theta(\eta,\tau) - \theta_\infty) - \delta B_0^2 v(\eta,\tau) \tag{1}$$

the energy equation in the absence of radiation is presented as under.

$$\rho c_p \frac{\partial \theta(\eta,\tau)}{\partial \tau} = k \frac{\partial^2 \theta(\eta,\tau)}{\partial \eta^2}, \tag{2}$$

subject to

$$\left.\begin{array}{ll} v(\eta,0) = 0, & \theta(\eta,0) = \theta_\infty \\ v(0,\tau) = A\tau^2, & v(\infty,\tau) = 0 \\ \theta(0,\tau) = \theta_w, & \theta(\infty,\tau) = \theta_\infty \end{array}\right\}, \tag{3}$$

The below given dimensionless variables

$$v^* = \frac{v}{\left(\nu^2 A\right)^{\frac{1}{5}}},\ \eta^* = \frac{\eta A^{\frac{1}{5}}}{\nu^{\frac{3}{5}}},\ \tau^* = \frac{\tau A^{\frac{2}{5}}}{\nu^{\frac{1}{5}}},\ \ \theta^*(\eta,\tau) = \frac{\theta - \theta_\infty}{\theta_w - \theta_\infty},$$

are incorporated into Eqs. (1–3). The momentum equation is given in Eq. (1) is nondimensionalized and is presented as under.

$$\frac{\partial v(\eta,\tau)}{\partial \tau} = \frac{\partial^2 v(\eta,\tau)}{\partial \eta^2} + Gr\theta(\eta,\tau) - H_a v(\eta,\tau), \tag{4}$$

The heat equation, which was displayed in dimensional form as Eq. (2) is now given in nondimensional form as under.

$$\Pr \frac{\partial \theta}{\partial \tau} = \frac{\partial^2 \theta}{\partial \eta^2}. \tag{5}$$

With non-similar initial and boundary conditions as:

$$\left.\begin{array}{lll} v(\eta,0) = 0, & v(0,\tau) = \tau^2, & v(\infty,\tau) = 0 \\ \theta(0,\tau) = 1, & \theta(\infty,\tau) = 0 & \theta(\eta,0) = 0 \end{array}\right\}, \tag{6}$$

where

$$Gr = \frac{g\beta_\theta \Delta\theta}{A^{\frac{3}{5}} \upsilon^{\frac{1}{5}}},\ H_a = \frac{\delta}{\rho} B_0^2 A^{-\frac{2}{5}} \upsilon^{\frac{1}{5}},\ \Pr = \frac{\mu c_p}{k}$$

Entropy generation. In heat transfer systems, using Eq. (4–6), the reduction in energy losses can be mathematically expressed[4–6,13,14].

$$E_{gen} = \frac{K}{\theta_\infty^2}\left(\frac{\partial \theta}{\partial \eta}\right)^2 + \frac{\mu}{\theta_\infty}\left(\frac{\partial v}{\partial \eta}\right)^2 + \frac{\delta \beta_0^2}{\theta_\infty} v^2. \tag{7}$$

Taking into consideration, the non-similarity variable, $\partial\theta/\partial\eta = \Delta\theta A^{\frac{1}{5}} \nu^{-\frac{3}{5}} \partial\theta^*/\partial\eta^*$ and $\partial v/\partial y = A^{\frac{2}{5}} \nu^{-\frac{1}{5}} \partial v^*/\partial\eta^*$ are produced and incorporated into Eq. (7), which yields

$$N_s = \frac{E_{gen}}{E_0} = \left[\left(\frac{\partial \theta}{\partial \eta}\right)^2 + \frac{B_r}{\Omega}\left(\frac{\partial v}{\partial \eta}\right)^2 + \frac{B_r}{\Omega} H_a v^2\right], \tag{8}$$

where

$$N_s = \frac{E_{gen} \nu^{\frac{6}{5}} \theta_\infty^2}{k A^{2/5} (\Delta\theta)^2},\ Br = \frac{\mu A^{\frac{2}{5}} \nu^{\frac{4}{5}}}{k\Delta\theta},\ \Omega = \frac{\Delta\theta}{\theta_\infty} = \frac{\theta_w - \theta_\infty}{\theta_\infty}.$$

Bejan number. The Bijan number for the dimensionless system developed in Eqs. (4–6) is defined as

$$B_e = \frac{\frac{K}{\theta_\infty^2}\left(\frac{\partial \theta}{\partial \eta}\right)^2}{\frac{K}{\theta_\infty^2}\left(\frac{\partial \theta}{\partial \eta}\right)^2 + \frac{\mu}{\theta_\infty}\left(\frac{\partial v}{\partial \eta}\right)^2 + \frac{\delta \beta_0^2}{\theta_\infty} v^2} \tag{9}$$

and

$$B_e = \frac{\left(\frac{\partial \theta}{\partial \eta}\right)^2}{\left(\frac{\partial \theta}{\partial \eta}\right)^2 + \frac{B_r}{\Omega}\left(\frac{\partial v}{\partial \eta}\right)^2 + \frac{B_r}{\Omega} H_a v^2} \tag{10}$$

Exact solutions by Laplace transform method. In the literature, numerical or approximate methods are used to deal with mixed convection problems, and the exact solutions are rare. Here, the exact solution can be obtained via the Laplace transformation method, (4–6) gives by applying the Laplace transformation:

$$q\overline{v}(\eta,q) = \frac{\partial^2 \overline{v}(\eta,q)}{\partial \eta^2} + Gr\overline{\theta}(\eta,q) - H_a \overline{v}(\eta,q) \tag{11}$$

The initial condition is used while applying the integral transform and the boundary conditions in the transformed variable are given as under.

$$\overline{v}(0,q) = \frac{2}{q^3}, \quad \overline{v}(\infty,q) = 0 \tag{12}$$

In the transformed variable the energy equation whit boundary conditions are given as:

$$\Pr q\overline{\theta}(\eta,q) = \frac{\partial^2\overline{\theta}(\eta,q)}{\partial\eta^2} \tag{13}$$

$$\overline{\theta}(0,q) = \frac{1}{q}, \quad \overline{\theta}(\infty,q) = 0 \tag{14}$$

Equation (13) can be solved by using boundary conditions (14) as:

$$\overline{\theta}(\eta,q) = \frac{e^{-\eta\sqrt{\Pr q}}}{q} \tag{15}$$

The inverting the Laplace transform is employed which yield to

$$\theta(\eta,\tau) = erfc\left(\frac{\eta\sqrt{\Pr}}{2\sqrt{\tau}}\right). \tag{16}$$

Meanwhile, Eq. (11) is solved taking into account Eqs. (11, 12, 15) yield to

$$\overline{v}(\eta,q) = \frac{2}{q^3}e^{-\eta\sqrt{q+\mathrm{H}_a}} - \frac{a}{q(q+a_0)}e^{-\eta\sqrt{q+\mathrm{H}_a}} + \frac{a}{q(q+a_0)}e^{-\eta\sqrt{\Pr}\sqrt{q}} \tag{17}$$

where $\Pr \neq 1$.

$$a = \frac{Gr}{1-\Pr},\ a_0 = \frac{\mathrm{H}_a}{1-\Pr}.$$

with the inverse Laplace transform,

$$v(\eta,\tau) = v_1(\eta,\tau) + v_2(\eta,\tau) + v_3(\eta,\tau) \tag{18}$$

where

$$v_1(\eta,\tau) = 2\left[\left(\frac{\tau^2}{4} - \frac{\eta}{16}\sqrt{\frac{1}{\mathrm{H}_a}}\right)e^{-\eta\sqrt{\mathrm{H}_a}}erfc\left(\frac{\eta}{2}\sqrt{\frac{1}{\tau}} - \sqrt{\mathrm{H}_a\tau}\right) - \left(\frac{\tau^2}{4} + \frac{\eta}{16}\sqrt{\frac{1}{\mathrm{H}_a}}\right)e^{\eta\sqrt{\mathrm{H}_a}}erfc\left(\frac{\eta}{2}\sqrt{\frac{1}{\tau}} + \sqrt{\mathrm{H}_a\tau}\right)\right]$$

]]><![CDATA[

$$v_2(\eta,\tau) = \frac{a}{a_0}\left[\begin{array}{l}\frac{e^{-a_0\tau}}{2}\left(e^{-\eta\sqrt{(\mathrm{H}_a-a_0)}}erfc\left(\frac{\eta}{2}\sqrt{\frac{1}{\tau}} - \sqrt{(\mathrm{H}_a-a_0)\tau}\right) + e^{\eta\sqrt{(\mathrm{H}_a-a_0)}}erfc\left(\frac{\eta}{2}\sqrt{\frac{1}{\tau}} + \sqrt{(\mathrm{H}_a-a_0)\tau}\right)\right) \\ -\frac{1}{2}\left(e^{-\eta\sqrt{\mathrm{H}_a}}erfc\left(\frac{\eta}{2}\sqrt{\frac{1}{\tau}} - \sqrt{\mathrm{H}_a\tau}\right) + e^{\eta\sqrt{\mathrm{H}_a}}erfc\left(\frac{\eta}{2}\sqrt{\frac{1}{\tau}} + \sqrt{\mathrm{H}_a\tau}\right)\right)\end{array}\right]$$

]]><![CDATA[

$$v_3(\eta,\tau) = \frac{a}{a_0}\left[erfc\left(\frac{\eta}{2}\sqrt{\frac{\Pr}{\tau}}\right) - \frac{e^{a_0\tau}}{2}\left(e^{-\eta\sqrt{-a_0\Pr}}erfc\left(\frac{\eta}{2}\sqrt{\frac{\Pr}{\tau}} - \sqrt{-a_0\tau}\right) + e^{\eta\sqrt{-a_0\Pr}}erfc\left(\frac{\eta}{2}\sqrt{\frac{\Pr}{\tau}} + \sqrt{-a_0\tau}\right)\right)\right] \tag{19}$$

Skin friction. The skin friction of the system in dimensionless form is given by

$$c_f = \left.\frac{\partial v(\eta,\tau)}{\partial\eta}\right|_{\eta=0} \tag{20}$$

Nusselt number. From Eq. (15) the Nusselt number in e dimensionless form is given by

$$Nu = \left.\frac{\partial\theta(\eta,\tau)}{\partial\eta}\right|_{\eta=0} \tag{21}$$

Ha	Gr	V
0.5	1	0.4067
–	–	0.3562
1	–	0.3919
0.5	–	0.4937
–	2	0.0190

Table 1. Finite difference results for velocity.

Ha	Gr	c_f
0.5	1	0.0105
–	–	0.0094
1	–	0.0106
0.5	–	0.0105
–	2	0.0141

Table 2. Finite difference results for skin-friction.

Ha	Gr	Be
0.5	1	$1.0961 \times e^{-6}$
–	–	$1.9870 \times e^{-6}$
1	–	$1.1753 \times e^{-6}$
0.5	–	$9.8233 \times e^{-7}$
–	2	$1.0484 \times e^{-6}$

Table 3. Finite difference results for Bejan number.

Results and discussion

A new problem of entropy generation is studied in this work numerically as well as analytically. The flow is considered over quadratic accelerated plate in the presence of a strong magnetic field. Analytical part of this work is done via Laplace transform whereas the numerical part is done using the finite difference scheme. Results for different parameters are computed and displayed in various plots and tables. The finite difference scheme results are computed using MATLAB.

Finite difference scheme. Finite difference method is a distinguished technique in the numerical analysis. This technique is applied here to compute results shown in tabular form. In this condition, the numerical solution which is identified exclusively at a finite number of points in the physical field is recognized as discrete. The operator of this numerical technique can pick the number of those points. In fact, both resolution and numerical solution precision are enhanced when the point number rises. The discrete approximation leads to a group of algebraic equations which are assessed according to the values of the discrete unknowns.

The assortment of positions where the discrete solution is calculated is recognized as the mesh. The fundamental basis of the finite-difference method is to substitute continuous derivatives by the supposed difference formulas which include only the discrete values related to locations on the mesh. The application of the finite-difference method to a differential equation implicates substituting all derivatives with difference formulas. Both derivatives with respect to space and derivatives with respect to time exist in the heat equation. Several systems can be obtained after varying the arrangement of mesh points in the difference formulas. Therefore, The numerical solution achieved via whatever valuable scheme will approximate the real solution to the original differential equation.

The above finite difference scheme, has been used for computing the following tabulated data. Therefore, Tables 1, 2, 3 and 4 are formed. The numerical values given in Table 1 shows the variation in velocity of the fluid. These results shows that increasing values of Ha causes the velocity water to decrease. However, increasing Gr decreases fluid velocity and the fluid flows slowly. Variation in the skin-friction for different values of Ha and Gr are shown in Table 2. From this table we can clearly see that increasing Ha results a decrease in the magnitude of skin-friction. However, skin-friction increases for larger values of Gr. Table 3 shows variation in the Bejan number for Ha and Gr when other parameters are kept constant. With increasing Ha, Bejan number increases but decreases for increasing Gr. The finite difference results for entropy generation are shown in Table 4. This table clearly shows that with increasing Ha, entropy generation decreases. However, for larger values of Br and Ω, entropy generation increases.

Ha	τ	Br	Ω	Pr	Gr	η	Ns
0.5	2	0.5	10	6.2	1	0.5	0.1907
1	–	–	–	–	–	–	0.1878
0.5	–	0.9	–	–	–	–	0.343
–	–	0.5	15	–	–	–	0.1272
–	–	–	10	–	–	–	0.1985

Table 4. Finite difference results for entropy generation.

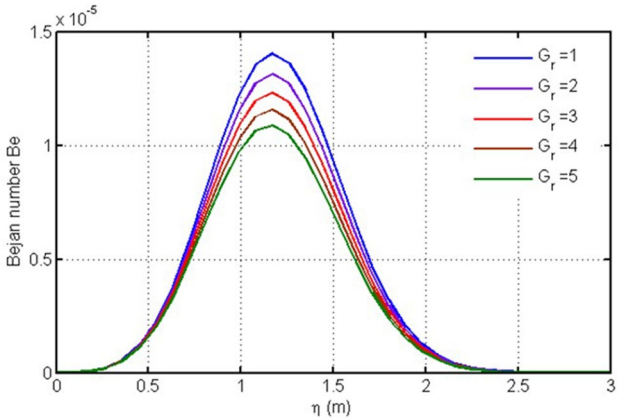

Figure 1. Plot for Bejan number versus η against Gr.

Numerical simulations of exact solutions. In Fig. 1, Bejan number is plotted against the space variable η for different values of Grashof number. It is clear from this figure that Gr is responsible for lowering Bejan number.

In the subsequent figure (Fig. 2), Bejan number versus η is examined for magnetic parameter (Ha), also knows as Hartmann number. It is found that Ha cause Bejan number to grow, however, the increase in Bejan number due to Ha is more dominant.

Figure 3 shows plot for entropy generation versus η against Gr. In this figure the variation in entropy generation profile is shown for different values of Thermal Grashof number, the greater this value, the higher is the entropy generation and vice versa. Physically the higher values Gr enhances the irreversibility. Figure 4 is plotted for entropy generation versus η against Ha. Entropy generation behaves in opposite manner for the larger values of Ha i.e. decreasing with increasing Ha (Fig. 4) due to prominent friction force.

The velocity profile for different values of Gr is plotted in this figure (Fig. 5). Due to buoyancy forces the velocity decreases with the increasing values of Grashof number. This purpose is served by varying the Grashof number (Gr) while other parameters possess some constant values. Gr is a critical quantity in those ow problems which involve the free convection mechanism. The physical phenomenon causing such results is an augmentation in the wall temperature due to a rise in Gr. This leads to reduce the force of internal resistance and makes gravitational effects more strong. Correspondingly, the viscous influence on the velocity is efficiently encountered by the buoyancy force and the flow field species a rising trend.

Figure 6 is plotted to illustrate the velocity field for several values of the magnetic parameter Ha, (Hartmann number). It is noticed that Ha produces decelerating effects on the fluid motion. Physically, Newtonian fluid acquires maximum transportation speed in the absence of magnetic influence. The physical argument that justifies this flow retardation is the origination of the Lorentz force. According to Lorentz's theory, this force is a resistive one, which serves against the flow direction. Moreover, as Ha increases, this force enhances the viscous effects and drags the viscous fluid in a reverse direction.

Figure 7 is plotted for velocity versus η against *time*. It is found that velocity increases with increasing time near the plate, however, for values away from the plate, goes to zero.

Figure 8 is plotted for temperature versus η against Pr. For different values of time this figure is plotted. Here it is noticed that the obtained solutions are satisfying the imposed conditions on the boundary. For different Pr the temperature profile is drawn in this figure. From $Pr = 1$ to $Pr = 4$ the temperature in showing increasing behavior.

The skin friction against time (t) is plotted in this figure (Fig. 9) for various values of Ha, it is clearly seen from this plot that skin friction is decreasing for increasing values of Ha. Fig. 10 is plotted for skin-friction versus time against Gr, when other parameters possess some constant values. Gr is a critical quantity in such a flow problem which involves the free convection mechanism, and with its increasing values skin-friction decreases. Physically, for different values of Gr the skin friction is showing decreasing behavior as contrary to velocity due to weaker contact. However, the change is very small to clearly differentiate.

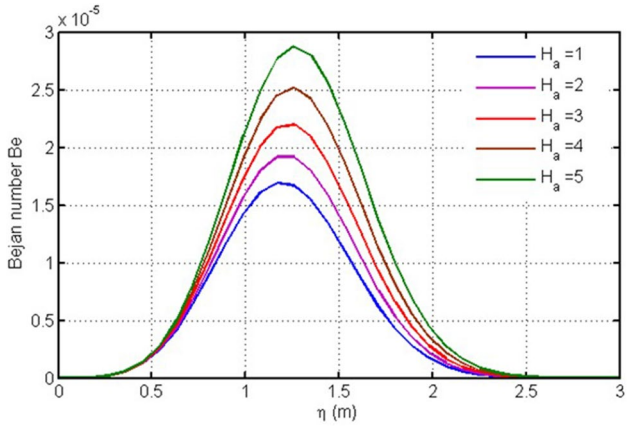

Figure 2. Plot for Bejan number versus η against *Ha*.

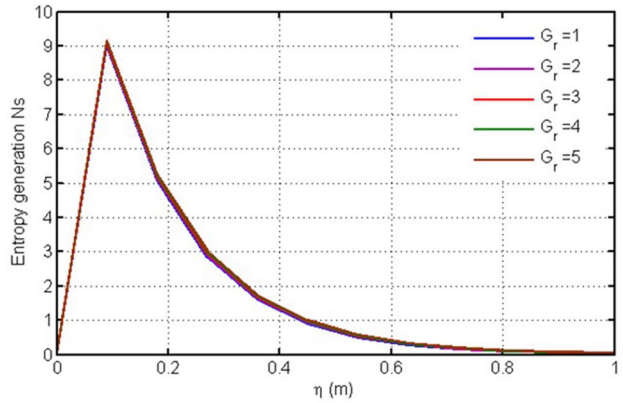

Figure 3. Plot for entropy generation versus η against *Gr*.

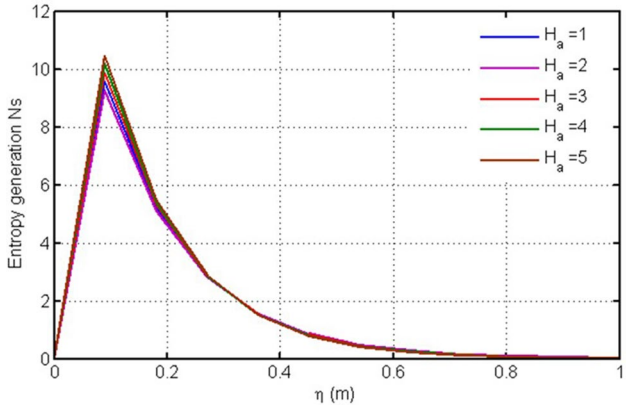

Figure 4. Plot for entropy generation versus η against *Ha*.

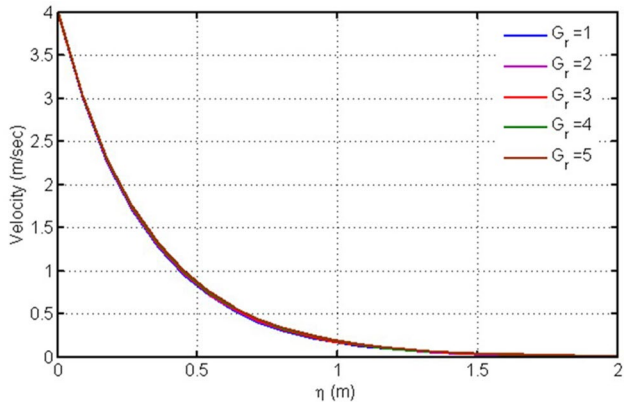

Figure 5. Plot for velocity versus η against *Gr*.

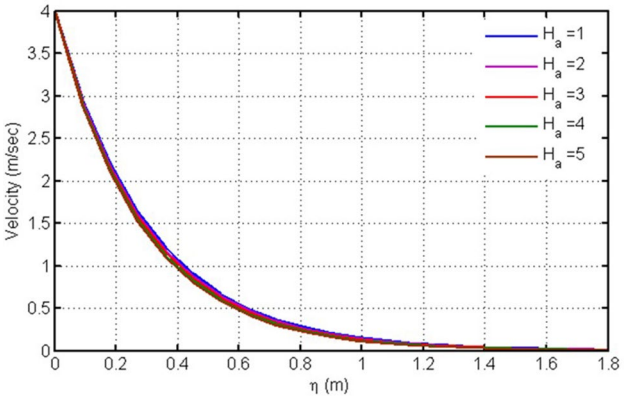

Figure 6. Plot for velocity versus η against *Ha*.

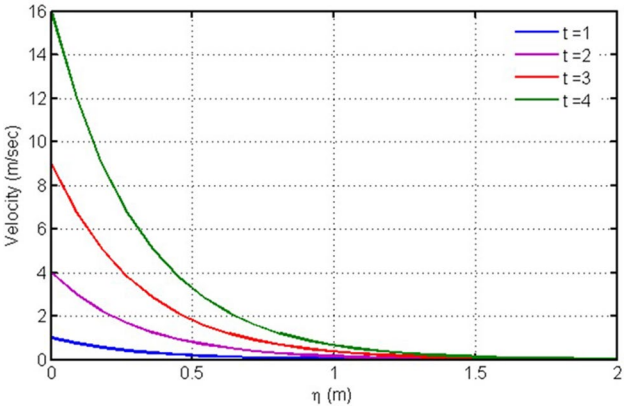

Figure 7. Plot for velocity versus η against *time*.

For various values of Pr the Nusselt number is drawn in this figure (Fig. 11) against time. Near the plate the Nusselt number decreases with increasing values of time while away from the plate the Nusselt number increases with increasing values of Pr.

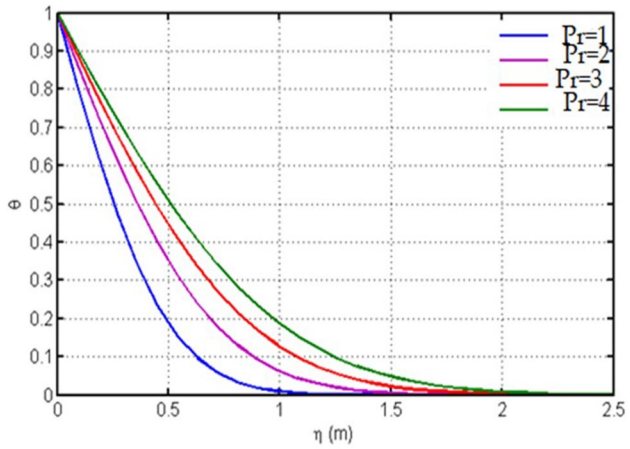

Figure 8. Plot for temperature versus η against Pr.

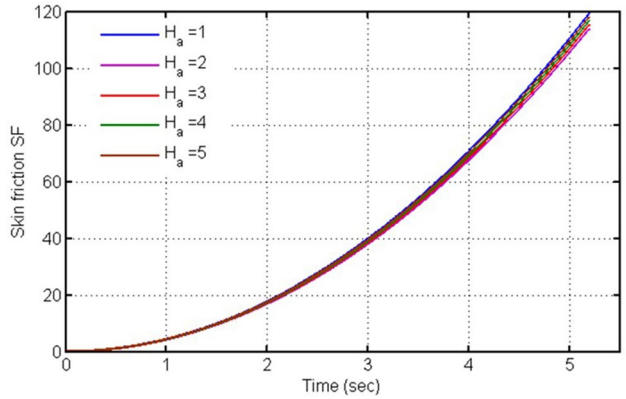

Figure 9. Plot for skin-friction versus time against Ha.

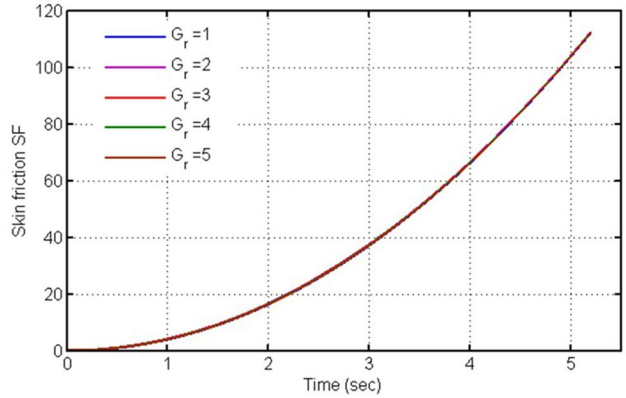

Figure 10. Plot for skin-friction versus time against *Gr*.

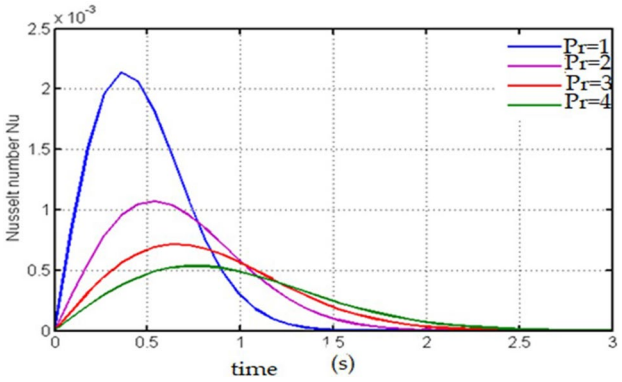

Figure 11. Plot for Nusselt number versus time against Pr.

Concluding remarks

In this work, the effect of magnetic field is studied on highly accelerated fluid motion and the the entropy generation analysis is then performed by taking water as a Newtonian fluid. The fluid is constantly heated from one side and heat transfers due to convection. The problem is first modelled and then solved for exact and numerical solutions. Results for Bejan number, entropy generation, velocity, temperature, and skin-friction are computed in tables and various plots. The following key points are concluded from this work.

- Entropy generation decreases with increasing Ha but increases for larger values of Br and Ω.
- Ha reduces fluid motion.
- With increasing Ha, Bejan number increases but decreases for increasing Gr.
- The variation in the Bejan number is more visible compare to entropy generation for larger values of Gr.
- The magnitude of entropy generation is bigger compare to Bejan number for greater Hartman number, however, this change in Bejan number is more effective.

Received: 21 February 2021; Accepted: 20 April 2021
Published online: 07 June 2021

References

1. Bejan, A. *Heat Transfer* (Wiley, 1993).
2. Bejan, A. *Advanced Engineering Thermodynamics* (Wiley, 1997).
3. Bejan, A. A study of entropy generation in fundamental convective heat transfer. *J. Heat Transf.* **101**(4), 718–725 (1979).
4. Bejan, A. Second law analysis in heat transfer. *Energy* **5**, 720–732 (1980).
5. Bejan, A. Second-law analysis in heat transfer and thermal design. In *Advances in Heat Transfer* 1–58 (Elsevier, 1982).
6. Bejan, A. *Entropy Generation Minimization: The Method of Thermodynamic Optimization of Finite-Size Systems and Finite-Time Processes* (CRC Press, 1995).
7. Bejan, A., Tsatsaronis, G. & Moran, M. J. *Thermal Design and Optimization* (Wiley, 1995).
8. Bejan, A. *Entropy Generation Minimization: The Method of Thermodynamic Optimization of Finite-Size Systems and Finite-Time Processes* (CRC Press, 2013).
9. Awad, M. M. A new definition of Bejan number. *Therm. Sci.* **16**, 1251–1253 (2012).
10. Saouli, S. & Aïboud-Saouli, S. Second law analysis of laminar falling liquid film along an inclined heated plate. *Int. Commun. Heat Mass Transf.* **31**, 879–886 (2004).
11. Sheremet, M. A., Oztop, H. F., Pop, I. & Abu-Hamdeh, N. Analysis of entropy generation in natural convection of nanofluid inside a square cavity having hot solid block: Tiwari and Das' model. *Entropy* **18**, 9 (2016).
12. Ji, Y., Zhang, H.-C., Yang, X. & Shi, L. Entropy generation analysis and performance evaluation of turbulent forced convective heat transfer to nanofluids. *Entropy* **19**, 108 (2017).
13. Qing, J., Bhatti, M. M., Abbas, M. A., Rashidi, M. M. & Ali, M.E.-S. Entropy generation on MHD Casson nanofluid flow over a porous stretching/shrinking surface. *Entropy* **18**, 123 (2016).
14. Sheikholeslami, M., Arabkoohsar, A., Khan, I., Shafee, A. & Li, Z. Impact of Lorentz forces on Fe_3O_4-water ferrofluid entropy and exergy treatment within a permeable semi annulus. *J. Clean. Prod.* **221**, 885–898 (2019).
15. Saqib, M., Ali, F., Khan, I., Sheikh, N. A. & Khan, A. Entropy generation in different types of fractionalized nanofluids. *Arab. J. Sci. Eng.* **44**, 531–540 (2019).
16. Khan, A. *et al.* Entropy generation in MHD conjugate flow with wall shear stress over an infinite plate: exact analysis. *Entropy* **21**, 359 (2019).
17. Hayat, T. *et al.* Impact of Cattaneo–Christov heat flux model in flow of variable thermal conductivity fluid over a variable thicked surface. *Int. J. Heat Mass Transf.* **99**, 702–710 (2016).
18. Hayat, T., Khan, S. A. & Alsaedi, A. Irreversibility characterization in nanoliquid flow with velocity slip and dissipation by a stretchable cylinder. *Alex. Eng. J.* **60**, 2835–2844 (2021).
19. Hayat, T., Khan, S. A., Alsaedi, A. & Zai, Q. Z. Computational analysis of heat transfer in mixed convective flow of CNTs with entropy optimization by a curved stretching sheet. *Int. Commun. Heat Mass Transf.* **118**, 104881 (2020).
20. Hayat, T., Khan, S. A., Khan, M. I. & Alsaedi, A. Theoretical investigation of Ree–Eyring nanofluid flow with entropy optimization and Arrhenius activation energy between two rotating disks. *Comput. Methods Programs Biomed.* **177**, 57–68 (2019).

21. Khan, M. I. Transportation of hybrid nanoparticles in forced convective Darcy–Forchheimer flow by a rotating disk. *Int. Commun. Heat Mass Transf.* **122**, 105177 (2021).
22. Khan, M. I. & Alzahrani, F. Cattaneo–Christov Double Diffusion (CCDD) and magnetized stagnation point flow of non-Newtonian fluid with internal resistance of particles. *Phys. Scr.* **95**, 125002 (2020).
23. Khan, M. I. & Alzahrani, F. Nonlinear dissipative slip flow of Jeffrey nanomaterial towards a curved surface with entropy generation and activation energy. *Math. Comput. Simul.* **185**, 47–61 (2021).
24. Khan, M. I. & Alzahrani, F. Dynamics of activation energy and nonlinear mixed convection in Darcy–Forchheimer radiated flow of Carreau nanofluid near stagnation point region. *J. Therm. Sci. Eng. Appl.* **13**, 051009 (2021).
25. Khan, M. I. & Alzahrani, F. Free convection and radiation effects in nanofluid (silicon dioxide and molybdenum disulfide) with second order velocity slip, entropy generation, Darcy–Forchheimer porous medium. *Int. J. Hydrog. Energy* **46**, 1362–1369 (2021).
26. Khan, M. I., Waqas, M., Hayat, T. & Alsaedi, A. A comparative study of Casson fluid with homogeneous-heterogeneous reactions. *J. Colloid Interface Sci.* **498**, 85–90 (2017).
27. Khan, S. A., Hayat, T. & Alsaedi, A. Entropy optimization in passive and active flow of liquid hydrogen based nanoliquid transport by a curved stretching sheet. *Int. Commun. Heat Mass Transf.* **119**, 104890 (2020).
28. Khan, S. A., Hayat, T., Alsaedi, A. & Ahmad, B. Melting heat transportation in radiative flow of nanomaterials with irreversibility analysis. *Renew. Sustain. Energy Rev.* **140**, 110739 (2021).
29. Khan, S. A., Hayat, T., Khan, M. I. & Alsaedi, A. Salient features of Dufour and Soret effect in radiative MHD flow of viscous fluid by a rotating cone with entropy generation. *Int. J. Hydrog. Energy* **45**, 14552–14564 (2020).
30. Khan, S. A. *et al.* Entropy optimized CNTs based Darcy–Forchheimer nanomaterial flow between two stretchable rotating disks. *Int. J. Hydrog. Energy* **44**, 31579–31592 (2019).
31. Khalid, A., Khan, I., Khan, A. & Shafie, S. Unsteady MHD free convection flow of Casson fluid past over an oscillating vertical plate embedded in a porous medium. *Eng. Sci. Technol. Int. J.* **18**(3), 309–317 (2015).
32. Sheikh, N. A. *et al.* Comparison and analysis of the Atangana–Baleanu and Caputo–Fabrizio fractional derivatives for generalized Casson fluid model with heat generation and chemical reaction. *Results Phys.* **7**, 789–800 (2017).
33. Ali, F., Saqib, M., Khan, I. & Sheikh, N. A. Application of Caputo–Fabrizio derivatives to MHD free convection flow of generalized Walters'-B fluid model. *Eur. Phys. J. Plus* **131**(10), 377 (2016).
34. Shah, N. A. & Khan, I. Heat transfer analysis in a second grade fluid over and oscillating vertical plate using fractional Caputo–Fabrizio derivatives. *Eur. Phys. J. C* **76**(7), 362 (2016).
35. Ali, F., Sheikh, N. A., Khan, I. & Saqib, M. Impact of Lorentz forces on Fe3O4-water ferrofluid entropy and exergy treatment within a permeable semi annulus. *J. Clean. Prod.* **221**, 885–898 (2019).
36. Khalid, A., Khan, I. & Shafie, S. Exact solutions for free convection flow of nanofluids with ramped wall temperature. *Eur. Phys. J. Plus* **130**(4), 57 (2015).
37. Gul, A., Khan, I., Shafie, S., Khalid, A. & Khan, A. Heat transfer in MHD mixed convection flow of a ferrofluid along a vertical channel. *PLoS ONE* **10**(11), e0141213 (2015).
38. Khater, A. H., Callebaut, D. K. & Abdelhameed, T. N. Variational principles and stability criteria for spherically symmetric, gravitating, ideally magnetohydrodynamic configurations. *Nuovo Cimento B Ser.* **120**, 1313 (2005).
39. Khater, A. H., Callebaut, D. K. & Abdelhameed, T. N. Variational principles and stability criteria for two-dimensional, gravitating, ideal magnetohydrodynamic configuration. *Nuovo Cimento B Ser.* **121**(9), 995 (2006).
40. Khan, I., Abdelhameed, T. N. A. & Dennis, L. C. C. Heat transfer in eccentric-concentric rotation of a disk and fluid at infinity. *J. Comput. Theor. Nanosci.* **13**, 6482–6487 (2016).
41. Ahmed, T. N. & Khan, I. Mixed convection flow of sodium alginate (SA-NaAlg) based molybdenum disulphide (MoS_2) nanofluids: maxwell Garnetts and Brinkman models. *Results Phys.* **8**, 752–757 (2018).
42. Ahmed, T. N. & Khan, I. Entropy generation in $C_6H_9NAO_7$ fluid over an accelerated heated. *Front. Phys.* **7**, 1–9 (2020).
43. Haq, S. U., Khan, I., Ali, F., Khan, A. & Abdelhameed, T. N. A. Influence of slip condition on unsteady free convection flow of viscous fluid with ramped wall temperature. In *Abstract and Applied Analysis, 2015* (2015) Article ID 327975, 7 pages

Acknowledgment

The author would like to thank the Deanship of Scientific Research at Majmaah University for supporting this work under Project R-2021-99.

Author contributions

T.N.A. wrote this manuscript.

Competing interests

The author declares no competing interests.

Additional information

Correspondence and requests for materials should be addressed to T.N.A.

Reprints and permissions information is available at www.nature.com/reprints.

Publisher's note Springer Nature remains neutral with regard to jurisdictional claims in published maps and institutional affiliations.